Numerical computation of liquid metal MHD duct flows at finite magnetic Reynolds number

Vinodh Bandaru, Thomas Boeck, Dmitry Krasnov, Jörg Schumacher
Institute of Thermodynamics and Fluid Mechanics,
Technische Universität Ilmenau,
P.O.Box 100565, 98684 Ilmenau, Germany
Corresponding author : vinodh-kumar.bandaru@tu-ilmenau.de

Abstract. A coupled finite difference-boundary element computational procedure for the simulation of turbulent liquid metal flow in a straight rectangular duct in the presence of an externally imposed magnetic field at finite magnetic Reynolds number (R_m) is presented. Periodicity is assumed in the streamwise direction and the duct walls are considered to be perfectly insulating. Details of the algorithm for the coupled electromagnetic solution of the interior and exterior will be discussed along with laminar flow results using idealized pseudo-vaccum magnetic boundary conditions.

Introduction. Turbulent conducting flows at finite magnetic Reynolds numbers occur in magnetohydrodynamic turbulence in plasmas, and in the generation of magnetic fields by the dynamo effect. In simulations the former case is typically studied as box turbulence without walls, and the latter in a closed spherical fluid domain. We are interested in turbulent liquid-metal duct flows in the presence of an externally generated magnetic field, which is of interest for metallurgical applications such as in the continuous casting of steel and aluminum. It can be expected to show complex interactions between the magnetic field and the flow. Studies of these interactions also guide the quantification of the reaction time in the measurement of transient liqud metal flows through Lorentz force velocimetry.

The magnetic Reynolds number R_m is a measure of the relative magnitude of the induced secondary magnetic field to the imposed magnetic field. We focus on the computation of velocity and magnetic fields in the interior of the duct, in the regime of $R_m \sim 1$. Since the secondary magnetic field (which is significant) also pervades the space outside the duct, proper modelling of the magnetic field in the interior requires a consistent treatment of the magnetic field across the duct boundaries. This is typically done through either of the following two approaches. The first approach is to extend the computational domain to model the magnetic field also outside the fluid domain. The second approach is to model the magnetic field only inside the duct but with magnetic boundary conditions that arise from the boundary integral formulation of the exterior field. Extending the domain to the exterior is computationally costly and also inconvenient for the parallelization of an existing DNS code [1]. Furthermore, since the exterior secondary magnetic field in itself is not in our interest, we prefer the boundary integral approach.

Characterizing the exterior magnetic field by the boundary integral procedure gives rise to non-local boundary conditions [2]. Such boundary conditions typically arise in the non-spectral simulation of dynamo and astrophysical processes. A hybrid finite volume-boundary element computational procedure has been first proposed by Iskakov et al.[2, 3] and since then has been applied by various researchers to simulate kinematic problems wherein the velocity field is given and the evolution of the magnetic field is sought (see, e.g., [4, 5]). In this work, we attempt to perform a full dynamic simulation of the flow and magnetic fields evolving together in the case of an MHD duct flow. A numerical procedure for the full MHD solution along with laminar flow solutions with idealized magnetic boundary conditions will be presented.

Governing equations and numerical procedure We consider the incompressible flow of an electrically conducting fluid driven by a mean pressure gradient in a straight square duct with an imposed magnetic field $\boldsymbol{B}_0$. Flow crossing the magnetic field contributes to a current density $\boldsymbol{J}$ which forms the source of a secondary magnetic field $\boldsymbol{B}$ that acts as a perturbation to the primary imposed magnetic field. The total magnetic field $\boldsymbol{B}_T = \boldsymbol{B}_0 + \boldsymbol{B}$ interacts with the current density $\boldsymbol{J}$ to produce a Lorentz force $\boldsymbol{F} = \boldsymbol{J} \times \boldsymbol{B}_T$ which acts as a body force on the flow field. This body force affects the flow field which in turn affects the magnetic field. The physics of this coupled evolution of the velocity and magnetic fields is governed by the Navier-Stokes and the magnetic field transport equations respectively with the constraints of solenoidality of both the fields. Using U, L, L/U, ρU^2, B_0 and $\sigma U B_0$ as the scales for the velocity, length, time, pressure, magnetic field and current density respectively, the governing equations in the interior of the duct in non-dimensional form are

$$\frac{\partial \boldsymbol{v}}{\partial t} + (\boldsymbol{v} \cdot \nabla)\boldsymbol{v} = -\nabla p + \frac{1}{Re}\nabla^2 \boldsymbol{v} + \frac{N}{R_m}\left((\nabla \times \boldsymbol{b}_T) \times \boldsymbol{b}_T\right), \tag{1}$$

$$\nabla \cdot \boldsymbol{v} = 0, \tag{2}$$

$$\frac{\partial \boldsymbol{b}}{\partial t} + (\boldsymbol{v} \cdot \nabla)\boldsymbol{b}_T = (\boldsymbol{b}_T \cdot \nabla)\boldsymbol{v} + \frac{1}{R_m}\nabla^2 \boldsymbol{b}, \tag{3}$$

$$\nabla \cdot \boldsymbol{b} = 0, \tag{4}$$

$$u = v = w = 0 \quad \text{at } y, z = \pm 1, \quad \text{periodicity in } x \text{ direction} \tag{5}$$

where x, y and z denotes the streamwise, spanwise and wall normal directions respectively and all the lower case variables correspond to non-dimensional quantities. The mean cross-sectional velocity U, the half width of the channel L, and a characteristic value of the imposed magnetic field strength B_0 have been taken for non-dimensionlization. Parameters in the equations are the Reynolds number $Re \equiv UL/\nu$, the magnetic interation parameter $N \equiv Ha^2/Re$, where $Ha \equiv B_0 L \left(\sigma/\rho\nu\right)^{1/2}$ is the Hartmann number and the magnetic Reynolds number $R_m \equiv UL/\lambda$. The secondary magnetic field in the exterior of the duct is curl free and hence represented as the gradient of a scalar potential, $\boldsymbol{b} = -\nabla\psi$. The solenoidal condition leads to the governing equation in the exterior as

$$\nabla^2 \psi = 0 \tag{6}$$

The numerical solution is carried out on a non-uniform rectangular grid, with clustering of grid points near the walls to resolve the Hartmann layers and side layers that are characteristic of duct MHD flows. A collocated grid arrangement is used with the variables $\boldsymbol{v}$, p and $\boldsymbol{b}$ stored at the same grid points. A finite difference scheme with semi-implicit time stepping is used for the discretization of the momentum and the magnetic field transport equations, wherein the diffusive terms are treated in an implicit manner. For the momentum equation, a fractional time step procedure is adopted to first compute an intermediate velocity field that is in turn projected onto a solenoidal velocity field through a pressure correction step. Poisson equations for the intermediate velocities and pressure are transformed into the Fourier space with respect to x and are solved using the software package FISHPACK [6]. The mean pressure gradient is adjusted in order to obtain a constant volume flux in the duct. Details of the numerical scheme for the solution of the velocity field can be found in Krasnov et al. [1].

Semi-implicit discretization of Eq.(3) with further simplification yields

$$-f\boldsymbol{b}^{n+1} + \nabla^2 \boldsymbol{b}^{n+1} = -f\boldsymbol{q} \tag{7}$$

for the magnetic field perturbation at the current time step $n+1$, where f is a discretization parameter and $\boldsymbol{q}$ contains the convective and field stretching terms at the previous time steps n and $n-1$. Since the domain is periodic in the streamwise direction, introducing the Fourier transform along the x-direction leads to

$$\boldsymbol{b}(x,y,z) = \sum_{k=-\frac{N_x}{2}}^{k=\frac{N_x}{2}-1} \hat{\boldsymbol{b}}(y,z) e^{i\alpha_k x} \tag{8}$$

where $\alpha_k = 2\pi k/L_x$ is the streamwise wavenumber, L_x being the length of the duct and N_x the number of grid points along the length of the duct. Substituting this in Eq.(7) and dropping the superscript yields

$$-(f+\alpha_k^2)\hat{\boldsymbol{b}} + \nabla_{yz}^2 \hat{\boldsymbol{b}} = -f\hat{\boldsymbol{q}} \tag{9}$$

which is to be solved for the Fourier coefficients $\hat{b}_x$, $\hat{b}_y$ and $\hat{b}_z$ in the interior of the duct. However, since Eq.(4) acts as an additional constraint on the magnetic field and overdetermines the sytem along with Eq.(3), we solve Eq.(9) only for the components $\hat{b}_y$ and $\hat{b}_z$ and reconstruct the component $\hat{b}_x$ from the condition

$$\hat{b}_x = \frac{-1}{i\alpha_k}\left(\frac{\partial \hat{b}_y}{\partial y} + \frac{\partial \hat{b}_z}{\partial z}\right),\ k \neq 0 \tag{10}$$

In this way the solenoidal property of the resulting magnetic field is preserved. For the mode with $k=0$, the component $\hat{b}_x$ is decoupled from the other two components and hence Eq.(9) is used to compute $\hat{b}_x$ with Dirichlet boundary conditions. The magnetic field in the real space is recovered from the Fourier components $\hat{b}_x$, $\hat{b}_y$ and $\hat{b}_z$ through the inverse Fourier transform.

Evaluation of the components $\hat{b}_y$ and $\hat{b}_z$ at each wavenumber requires boundary conditions that are consistent with the exterior field, the formulation of which is described here. The Fourier representation of Eq.(6) leads to the Helmholtz equation $(\nabla_{yz}^2 - \alpha_k^2)\hat{\psi} = 0$, which using the Green's second identity can be represented in the boundary integral form as

$$c\hat{\psi}(\boldsymbol{r'}) = \text{P.V.} \oint [G(\boldsymbol{r'},\boldsymbol{r})\hat{b_n}(\boldsymbol{r}) + \hat{\psi}(\boldsymbol{r})\frac{\partial G}{\partial n}(\boldsymbol{r'},\boldsymbol{r})] dl(\boldsymbol{r}) \tag{11}$$

for the values of $\hat{\psi}$ on the rectangular boundary, where n represents the boundary normal direction, $G(\boldsymbol{r'},\boldsymbol{r})$ is the Green's function of the Helmholtz operator [7] about the pole $\boldsymbol{r'} = y\boldsymbol{e}_y + z\boldsymbol{e}_z$ and the integration along the rectangular contour is in the sense of a Cauchy principal value. Eq.(10) is non-local in nature and is discretized using the boundary element method [8]. This involves dividing the rectangular contour into a number of small line elements called boundary elements (see Figure 1) and approximating the integral equation as the sum of integrals along each of these boundary elements. The grid points that store the variables lie at the ends of each of the elements and the variables $\hat{\psi}$ and $\hat{b_n}$ are assumed to be piecewise linear within each element. The integrals are evaluated numerically along all elements except at the pole using a four-point Gaussian quadrature in order to accurately account for the steep gradients in the Green's function. At the pole, the Green's function has a logarithmic singularity and

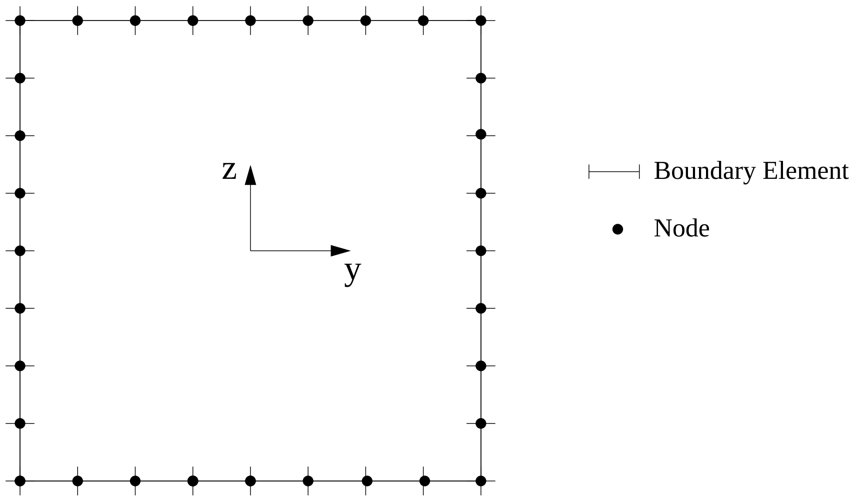

Figure 1: Grid with boundary elements and nodes used for the solution of the integral equation for $\hat{\psi}$.

is dealt with analytical integration over the element containing the pole. The boundary element discretization yields the discrete form of Eq.(11) which is a fully occupied linear system of equations $\boldsymbol{A}\hat{\boldsymbol{\psi}} = \boldsymbol{d}$ where $\boldsymbol{A}$ is a matrix and $\boldsymbol{d}$ a vector.

Eq.(12) along with $\hat{b}_\tau = -\frac{\partial \hat{\psi}}{\partial \tau}$ and the divergence free condition provides the boundary conditions for computing $\hat{b}_y$ and $\hat{b}_z$ from Eq.(9), which is solved by a coupled iterative procedure. The procedure is computationally intensive due to the fact that non-local boundary conditions translate into fully occupied linear systems unlike the sparse sytems that arise from local boundary conditions. The current density $\boldsymbol{j}$ is subsequently computed from the magnetic field $\boldsymbol{b}$ using the Ampère's law $\boldsymbol{j} = (\nabla \times \boldsymbol{b}_T)/R_m$.

Results and discussion. Simulations with pseudo vaccum magnetic boundary conditions were first performed in order to validate the solution of the magnetic field in the duct interior. For this purpose, it is assumed that for perfectly insulating walls, $j_n = 0$ is realized with vanishing tangential components of the magnetic field as

$$b_{\tau 1}, b_{\tau 2} = 0, \ \frac{\partial b_n}{\partial n} = 0 \quad \text{at } y, z = \pm 1 \tag{12}$$

the Neumann condition on b_n being obtained from Eq.(4). Starting with an initial laminar duct velocity profile and an imposed uniform magnetic field along the z-direction, the evolution of the velocity and magnetic fields is simulated at $R_m = 100$, until a steady state is reached. The contour of the streamwise velocity profile along with the corresponding magnetic field lines (in the x-z plane) are displayed in Figure 2.

It is observed that the velocity reaches the steady Hartmann-like profile through a series of oscillations that are damped eventually by diffusion, unlike the quasistatic regime which is diffusion dominated. These oscillatory states are remniscent of Alfvén waves that are typical of high R_m MHD flows. The corresponding stretching of the magnetic field lines is also observed.

Simulation of turbulent MHD duct flow with full treatment of the magnetic boundary conditions as described in the previous section along with detailed validation of the procedure using a quasistationary approach in the limiting case of low magnetic Reynolds number is in progress. Benchmarking of the procedure's numerical efficiency will be made with subsequent studies of MHD turbulence at finite magnetic Reynolds number.

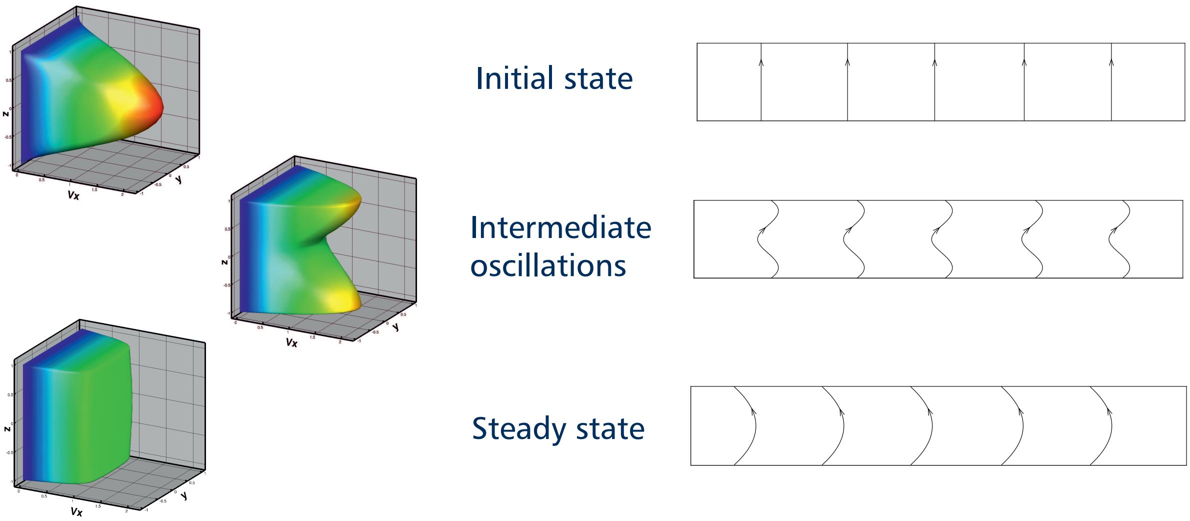

Figure 2: Contours of streamwise velocity profile at $Re = 2000$, $R_m = 100$, $Ha = 100$ in a cross-section (left). The corresponding magnetic field lines in the x-z plane, $y = 0$ (right). Grid size : $16 \times 128 \times 128$.

Acknowledgments. We acknowledge financial support from the Deutsche Forschungsgemeinschaft within the Research Training Group 1567.

References

[1] Krasnov, D., Zikanov, O. and Boeck, T.: Comparitive study of finite difference approaches in simulation of magnetohydrodynamic turbulence at low magnetic Reynolds number. Comp. Fluids 50 (2011) 46-59.

[2] Iskakov, A.B., Descombes, S. and Dormy, E.: An integro-differential formulation for magnetic induction in bounded domains: Boundary element finite volume method. J. Comp. Phy. 197 (2004) 540554.

[3] Iskakov, A., Dormy, E.: On magnetic boundary conditions for non-spectral dynamo simulations. Geophy. Astrophy. Fluid Dyn. 99-6 (2005) 481-492.

[4] Giesecke A., Stefani, F., Gerbeth, G. : Kinematic simulation of dynamo action by a hybrid boundary-element/finite-volume method. Magnetohydrodynamics 44 (2008) 237-252

[5] Gissinger C., Iskakov A., Fauve S., Dormy, E.: Effect of magnetic boundary conditions on the dynamo threshold of von Kármán swirling flows EPL 82 (2008) 29001.

[6] Adams J.C., Swarztrauber P., Sweet R. : Efficient fortran subprograms for the solution of separable elliptic partial differential equations. https://www2.cisl.ucar.edu/resources/legacy/fishpack.

[7] Stakgold, I. : *Boundary Value Problems of Mathematical Physics, Vol.2*, Macmillan (1968).

[8] Brebbia, C. and Walker, S.: *The Boundary Element Method for Engineers*, Pentech Press (1978).